

Identification of *O*-diglycosyl flavanones in *Fructus aurantii* by liquid chromatography with electrospray ionization and collision-induced dissociation mass spectrometry

Da-yong Zhou, Qing Xu, Xin-ya Xue, Fei-fang Zhang, Xin-miao Liang*

Biotechnology department, Dalian Institute of Chemical Physics, The Chinese Academy of Sciences, Dalian 116023, PR China

Received 22 November 2005; received in revised form 29 April 2006; accepted 8 May 2006

Available online 11 July 2006

Abstract

This study reported the application of LC–ESI/MS method to characterize *O*-diglycosyl flavanones of traditional Chinese medicine *Fructus aurantii*(Zhiqiao) and UPLC retention parameters method to expatiate the structure-retention relationship of these *O*-diglycosyl flavanones. The extract of *F. aurantii* was found containing neoeriocitrin, isonaringin, naringin, hesperidin, neohesperidin and neoponcirin. Tandem mass spectrometric method has been utilized to elucidate structure and differentiate the interglycosidic linkage of isomeric *O*-diglycosyl flavanones. Based on the relative abundance of fragments formed by fragmentation at glycosidic bonds in positive ion mode and CID MS spectra of deprotonated molecule $[M-H]^-$ in negative ion mode, the interglycosidic linkage of *O*-diglycosyl flavanones (flavonoid *O*-neohesperidosides and *O*-rutinosides, 1,2- and 1,6-) can be unambiguously differentiated. UPLC and a CSASS software were performed to obtain the retention parameters *a*, *c* and *k* values of these compounds. The Δa , Δc and α values within compound pair naringin to neoeriocitrin, neoponcirin to neohesperidin, naringin to isonaringin, neohesperidin to hesperidin, hesperidin to isonaringin, neohesperidin to naringin were calculated. We found there were some relationship between structure and retention parameters.

© 2006 Elsevier B.V. All rights reserved.

Keywords: LC–ESI/MS; *Fructus aurantii*; *O*-diglycosyl flavanones; UPLC; Retention parameters

1. Introduction

Flavonoids are very common and widespread secondary plant metabolites. It is estimated that about 2% of all carbon photosynthesized by plants, amounting to about 1×10^9 tonnes/year, is converted into flavonoids or related compounds [1]. The flavonoid family comprises 15 classes of compounds, including the flavones, flavonols, flavanones, chalcones, and isoflavones, etc. Although flavonoids are sometimes found as their aglycones, they most commonly occur in plant materials as glycosides. Sugar substitution on the flavonoid skeleton may occur through hydroxyl groups in the case of *O*-glycosides or directly to carbon atoms in A-ring in C-glycosides. The number of sugar rings substituted on the aglycone varies from one to four. Flavonoids have a wide range of biological and physiological activities and serve as chemotaxonomic marker compounds. Therefore, they have

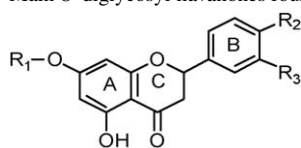
been extensively investigated in the past and during recent years. MS spectrometry, especially coupled to soft ionization-source such as atmospheric pressure chemical ionization (APCI) and electrospray ionization (ESI), which has advantage of sensitivity, possibilities of coupling with liquid chromatography and providing molecular mass and structural information on-line, so has become a very powerful tool in analysis of flavonoids. The tandem mass spectrometric fragmentation behaviors of flavonoid have been investigated extensively, and thus allow the identification of unknown compounds even when reference standards are unavailable.

Fructus aurantii (Zhi qiao) is a dried, closely mature fruit of *Citrus aurantium* L. As an important traditional Chinese medicine, *F. aurantii* shows bioactivities of anti-tumor [2], anti-hypertension [3], anti-shock [4], etc. Although *F. aurantii* has been proven effectively against tumor and hypertension via modern pharmacological studies and clinical trials, constituents of it have still not been studied well. In our antecedent studies [5], an LC–MS and CID MS/MS experiment was adopted to identify six *O*-diglycosyl flavanones from extracts of *F. aurantii*

* Corresponding author.

E-mail address: liangxm@dicp.ac.cn (X.M. Liang).

Table 1
Main *O*-diglycosyl flavanones found in *Fructus aurantii*



| No. | Compound | R1 | R2 | R3 | Mr |
|-----|------------------|----------------|----|------------------|-----|
| 1 | Neohesperidin(1) | Neohesperidose | OH | OH | 596 |
| 2 | Isonaringin(2) | Rutinose | H | OH | 580 |
| 3 | Naringin(3) | Neohesperidose | H | OH | 580 |
| 4 | Hesperidin(4) | Rutinose | OH | OCH ₃ | 610 |
| 5 | Neohesperidin(5) | Neohesperidose | OH | OCH ₃ | 610 |
| 6 | Neoponcirin(6) | Neohesperidose | H | OCH ₃ | 594 |

(the structure of them see Table 1). However, in the study, no standards were employed to validate the identification and the fragmentation patterns in negative mode did not be expatiated. Furthermore, the fragmentation patterns of target compounds in positive mode did not be explained thoroughly and the experimental data appeared to be too feeble to support the identification of the structures. Therefore, in this paper, a LC–MS and CID MS/MS experiment has been carried out to investigate the specific fragmentation patterns of the standard hesperidin (HES) and naringin (NAR). It will be discussed whether the specific fragmentation patterns of individual *O*-diglycosyl flavanone allow the identification of target compounds from the extract of *F. aurantii*. ESI was preferred in the present experiments since the target compounds in the *F. aurantii* samples were favorably analyzed with this ionization method.

In this paper, we also studied the structure-retention relationship of the *O*-diglycosyl flavanones found in *F. aurantii*. Lu et al. deduced the retention parameters equation in binary mobile phase system of RP-LC through thermodynamic methods [6,7]:

$$\ln k = a + cC_B$$

where k is retention factor ($k = (t_R - t_0)/t_0$); a , c are constants and relate to the structure in a given chromatographic system. C_B is the volume fraction of the solvent with higher solvent strength in the mobile phase. Based on this equation, Xinya Xue developed a software CSASS to calculate a , c values. Using the a , c values of target compound, we can predict the retention time (RT) of target compound in any chromatographic condition. The process to calculate a , c values is as follow: firstly, taking five times linear gradient UPLC experiments for a sample to obtain experimental retention time to every target compounds in different chromatographic condition. These five times linear gradients have the same initiative and final mobile phase composition but different gradient time. Secondly, each target compound is assigned an initial a , c value by experience. Thirdly, Euler's method is used to calculate predicted retention time using the initial a , c value. Finally, Levenberg–Marquardt method is used to calculate final a , c value. When input the experimental data of the five times linear gradient experiments into the software, the course of calculation is completed automatically. Comparing with conventional isocratic methods, these approaches can save

time to find the optimal separation condition and obtain more precise parameters. This software was utilized quite often in our research group to predict RT of target compounds and optimize chromatographic condition to complex system in RP-LC analysis, and the results very closed to the reality. In this paper, we use this method to obtain the a , c and α values of the *O*-diglycosyl flavanones identified in the extract of *F. aurantii*. We will discuss the relationship between structure and retention parameters thoroughly.

2. Materials and methods

2.1. Instrumentation

2.1.1. HPLC/DAD-MS

An Agilent 1100 Series LC/MSD Trap (USA) with a photodiode-array detector set at 280 nm (monitoring wavelength). Chromatographic conditions were as follow: column, Elite ODS₂ C₁₈ (Dalian, China), 250 mm × 4.6 mm, 5 μm; eluent: (A) water–formic acid (100:0.5, v/v), (B) acetonitrile–formic acid (100:0.5, v/v). The linear gradient was 0–40 min, 10–45% B; 40–45 min, 45–80% B. The flow-rate was 1 mL/min and the column temperature was 30 °C.

Mass range measured as 50–1000 amu. The spectra were acquired in both positive and negative modes; the ESI source conditions were adjusted as follow: drying N₂, temperature 350 °C, 8 L/min; nebulizing N₂, 2.4 Br. HPLC–MS connection was through an I.D. 0.007" tube. A 0.4 mL/min mobile phase was entered MS from outlet of DAD via splitting.

2.1.2. UPLC-TUV

An ACQUITY™ UPLC (Waters, USA) with a TUV detector set at 280 nm. Chromatographic conditions were as follow: column, ACQUITY UPLC™ BEHC₁₈ (Waters, USA), 100 mm × 2.1 mm, 1.7 μm; eluent: (A) water–formic acid (100:0.5, v/v), (B) acetonitrile–formic acid (100:0.5, v/v). The five times linear gradients for a , c values are shown in Table 2; the isocratic solvent composition to calculate k was 0–20 min, 20% B. The flow-rate was 0.25 mL/min and the column temperature was 30 °C; retention parameters were obtained and analyzed by the CSASS software.

2.2. Standard and reagents

Hesperidin and naringin were purchased from Sigma (USA) and Xiantong Time (China), respectively. The standards were diluted in acetonitrile to form a standards stock solution of

Table 2
Solvent composition of five times linear gradients

| | 10% B | 30% B |
|------------|-------|-------|
| Gradient 1 | 0 | 20 |
| Gradient 2 | 0 | 22 |
| Gradient 3 | 0 | 24 |
| Gradient 4 | 0 | 26 |
| Gradient 5 | 0 | 28 |

1 mg/mL, this solution was then diluted further in acetonitrile to form a standards work solution at 200 ng/mL before LC–MS analysis. Macroporous resin AB-8 (HG2-885-76) was purchased from TianJin Institute of Fine Chemistry (China). Acetonitrile (Merck, Germany), methonal (Yuwang, China) and formic acid (J&KCHEMICA, USA) were in HPLC grade. Reverse osmosis Milli-Q water (18.2 M Ω) (Millipore, USA) was used for all solutions and dilutions.

2.3. Plant material and sample preparation

F. aurantii were collected from Kai County, Chongqing city, China. The herb was authenticated by Institute of Medication, Xiyuan hospital of China Academy of traditional Chinese medicine. The sample was grounded into fine powder. A dry and fine powder of 5 g was weighed, 200 mL water–ethanol (20:80, v/v) was added, and the extraction was operated in an ultrasonic water bath for 30 min. The solution was filtered through 0.45 μ m cellulose membrane and the filtrate was dried with a rotary evaporator at 60 °C. Then the residual solid was collected and diluted in 5 mL water. A glass column (2 cm \times 50 cm) was wet-packed [8] with the macroporous resin (HG2-885-76). The bed volume (BV) of the resin was 50 mL. The sample was loaded into the adsorbate-laden column and was washed with 150 mL water firstly, and then was desorbed with 150 mL water–ethanol (20:80, v/v) solution. The eluent were concentrated and dried by rotary evaporator at 60 °C. The residual solid was diluted in 5 mL water–Acetonitrile (50:50, v/v) and was filtered through 0.22 μ m cellulose membrane before analysis.

2.4. Nomenclature

The nomenclature proposed by Domon and Costello [9] for glycoconjugates was adopted to denote the product ions of flavonoid glycosides (Scheme 1). Ions containing the aglycone are labeled $^{k,l}X_j$, Y_j and Z_j , where j is the number of the interglycosidic bond broken, counting from the aglycone, and the superscripts k and l indicate the cleavages within the carbohydrate rings. The glycosidic bond linking the glycan part to the aglycone is numbered 0. If the charge is retained on the carbohydrate residue, product ions are designated as $^{k,l}A_i$ and B_i , where i represents the number (≥ 1) of the glycosidic bond cleaved, counting from the non-reducing terminus. The nomenclature

proposed by Ma and Li [10] was followed to refer to product ions resulting from aglycone fragmentation. $^{m,n}A_0$ and $^{m,n}B_0$ are used to designate product ions containing intact A- and B-rings, respectively, where the superscripts m and n indicate the C-ring bonds that have been broken. The subscript 0 to the right of the letters A and B is used to avoid confusion with the A_i and B_i ($i \geq 1$) labels which are used to designate carbohydrate-related product ions.

2.5. Statistics

Statistical software SPSS 10.0 was adopted to accomplish paired-samples t -test.

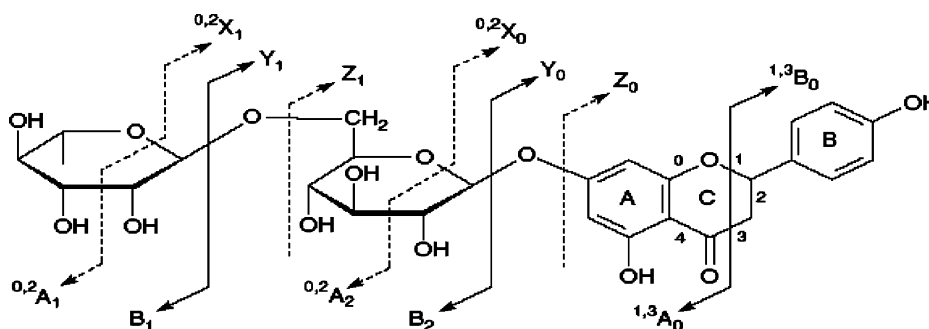
3. Results and discussion

3.1. Choice of interface

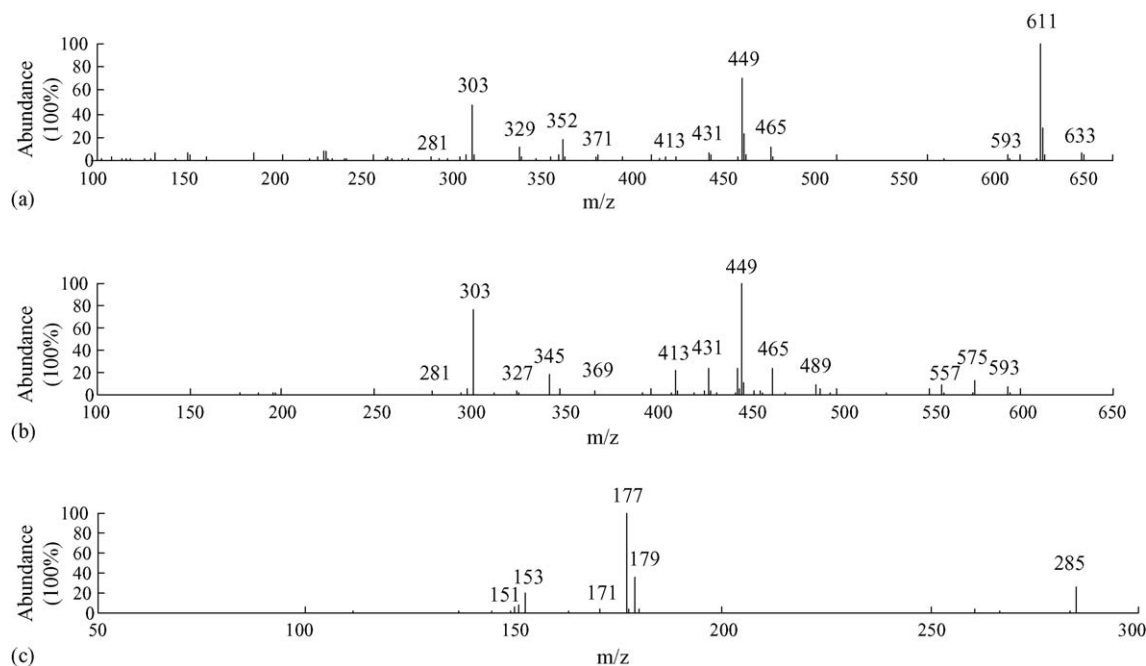
Our preliminary experiments showed that *O*-diglycosyl flavanones gave better response with ESI. For this reason, further experiments were carried out with the ESI source. The compounds were confirmed based on the molecular masses of the protonated species and their fragmentation patterns obtained by CID-MS of the protonated and deprotonated molecules. The dominant fragment ions were subsequently isolated in the ion trap and subjected to a second or third stage of collision to map the sequential fragmentation routes and provide additional structural information. The collision gas was nominally 1 mTorr helium, which is the standard buffer gas used in Ion-Trap MS.

3.2. MS experiments of standards hesperidin and naringin

The first order mass spectrum of hesperidin is shown in Scheme 2a. Four predominant product ions were observed which exhibits that the structure of hesperidin is not stable in ion-source and take place fragmentation. The four ions are the protonated molecule $[M+H]^+$ (m/z 611), the fragment ion $[Z_1+H]^+$ (m/z 449) correspond to the protonated molecule's loss of an glucose (162 u), the sodiated molecule $[M+Na]^+$ (m/z 633) and the protonated aglycone $[Y_0+H]^+$ (m/z 303) corresponded to the protonated molecule's loss of rhamnosylglucose (308u). The irregular Z_1 ion has been rationalized by loss of an glucose and a mechanism involving a



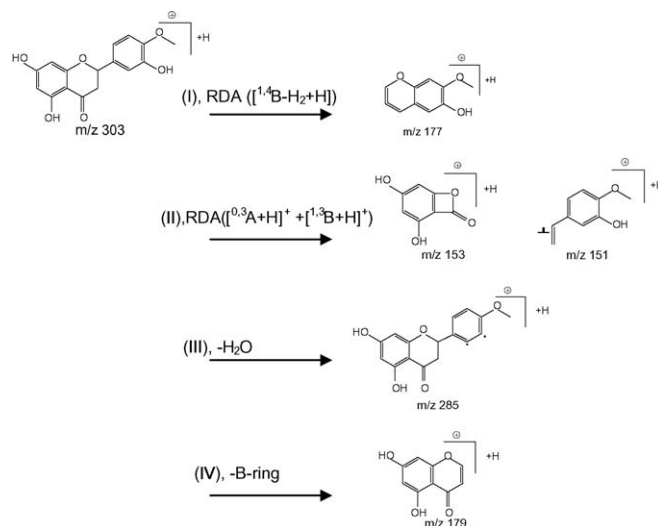
Scheme 1. Ion nomenclature followed for flavonoid glycosides (illustrated on naringenin 7-*O*-rutinoside).



Scheme 2. The mass spectra of hesperidin: (a) first order mass spectrum of hesperidin; (b) CID-mass spectrum of protonated molecule of hesperidin; (c) CID-mass spectrum of protonated aglycone of hesperidin.

mobile proton from the aglycone to the terminal rhamnose has been proposed [11]. The Z_1 ion has a markedly high relative abundance, which was unique as a flavanone 7-*O*-diglycosides [12,13]. The CID-MS product-ions spectrum of protonated hesperidin is shown in Scheme 2b. The product-ions $[Y_1+H]^+$ (m/z 465) formed by loss of terminal rhamnose, the product-ions $[Z_1+H]^+$ and $[Y_0+H]^+$ are observed synchronously. Additional peaks can be seen at m/z 593($[M-H_2O+H]^+$), 575($[M-2H_2O+H]^+$), 557($[M-3H_2O+H]^+$), 431($[Z_1-H_2O+H]^+$), 413($[Z_1-2H_2O+H]^+$), 345($[^{0,2}X_0+H]^+$). Scheme 2c illustrates the CID-MS product-ions spectrum of the aglycone of hesperidin. The product-ion species are formed in four fragmentation pathways (see Scheme 3). Pathway I involves a retro-Diels-Alder (RDA) fragmentation wherein bonds 1 and 4 undergo scission leading to the formation of the $[^{1,4}B-H_2+H]^+$ ions of m/z 177 as base peak. This fragmentation pathway was seldom reported in literatures as main fragmentation pattern of flavanone aglycones, and the product-ion maybe takes place retrocyclisation. Pathway II involves a RDA fragmentation wherein bonds 1 and 3 undergo scission leading to the formation of the $[^{1,3}A_0+H]^+$ and $[^{1,3}B+H]^+$ ions of m/z 153 and m/z 151, respectively. The $[^{1,3}A_0+H]^+$ ion is observed for all flavonoid groups, and is generally the fragment most readily formed then often constitutes the most abundant fragment ion [14]. The ion $[^{1,3}A_0+H]^+$ is the most useful fragment in terms of aglycone identification, for it provides information on the number and type of substituents in the A-ring. Pathway III indicates the neutral loss of H_2O from protonated molecular, which is a fragment commonly observed [14]. Pathway IV involves a fragmentation wherein bonds C-ring and B-ring undergo scission leading to the formation of the $[A_0-B\text{-ring}]^+$ ion of m/z 179. Though seldom reported, the pathway undergoing neutral

loss of intact B-ring is the most useful fragmentation in terms of aglycone identification, for which provides information on the number and type of substituents in B-ring. Curiously, the protonated molecular does not show prominent loss of CH_3 (15u), which is easily detected from the precursor-ion in methoxy group [15–17]. The MS information of naringin is summarized in Tables 3 and 4. Naringin has nearly the same fragmentation pattern as hesperidin. The mutual fragmentation pathways of them form the characteristic MSⁿ “fingerprint”. Using this “fingerprint”, we can screen and characterize target compounds in highly complex mixtures.



Scheme 3. Proposed characteristic fragmentation from the protonated aglycone of hesperidin.

Table 3
The first order ESI (+)-MS spectra date of peaks 1–6 (abundance% of ions are given)

| Peak No. | Identification | [M+H] ⁺ (m/z) | [M+Na] ⁺ (m/z) | [Y ₀ +H] ⁺ (m/z) | [Z ₁ +H] ⁺ (m/z) |
|----------|------------------|--------------------------|---------------------------|--|--|
| 1 | Neoeriocitrin(1) | 597(44.5) | 619(16.6) | 289(99.9) | 435(16.6) |
| 2 | Isonaringin(2) | 581(99.9) | 603(14.6) | 273(19.2) | 419(51.4) |
| 3 | Naringin(3) | 581(47.1) | 603(3.2) | 273(99.9) | 419(24.4) |
| 4 | Hesperidin(4) | 611(99.9) | 633(10.4) | 303(47.1) | 449(73.3) |
| 5 | Neohesperidin(5) | 611(40.5) | 633(3.2) | 303(99.9) | 449(35.0) |
| 6 | Neoponcirin(6) | 595(37.0) | – | 287(99.9) | 433(15.7) |

Table 4
The CID ESI (+)-MS spectra date of peaks 1–6 (abundance% of product-ions are given)

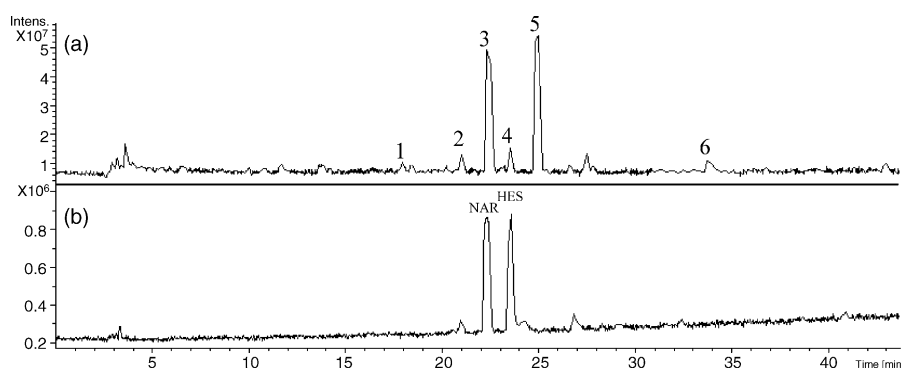
| Peak no. | 1 | 2 | 3 | 4 | 5 | 6 |
|--|------------------------|----------------------|-------------------|---------------------|------------------------|----------------------|
| Identification | Neoeriocitrin(1) (m/z) | Isonaringin(2) (m/z) | Naringin(3) (m/z) | Hesperidin(4) (m/z) | Neohesperidin(5) (m/z) | Neoponcirin(6) (m/z) |
| [M–H ₂ O+H] ⁺ | 579(3.9) | 563(10.9) | 563(7.7) | 593(7.1) | 593(8.0) | 577(107) |
| [M–2H ₂ O+H] ⁺ | 561(13.8) | 545(4.0) | 545(15.6) | 575(16.0) | 575(19.0) | 559(15.0) |
| [M–3H ₂ O+H] ⁺ | 543(16.9) | 527(10.7) | 527(19.5) | 557(14.0) | 557(21.2) | 541(16.0) |
| [M–4H ₂ O+H] ⁺ | 525(3.7) | 509(1.1) | 509(2.4) | 539(2.7) | 539(4.5) | 523(4.2) |
| [Z ₁ +H] ⁺ | 435(99.9) | 419(99.9) | 419(99.9) | 449(99.9) | 449(99.6) | 433(99.9) |
| [Y ₁ +H] ⁺ | 451(59.3) | 435(33.6) | 435(63.5) | 465(23.9) | 465(48.9) | 449(51.2) |
| [Z ₁ –H ₂ O+H] ⁺ | 417(26.5) | 401(18.0) | 401(15.8) | 431(28.4) | 431(17.8) | 415(25.5) |
| [Z ₁ –2H ₂ O+H] ⁺ | 399(22.4) | 383(13.3) | 383(23.0) | 413(18.1) | 413(16.3) | 397(15.8) |
| [^{0,2} X ₀ +H] ⁺ | 331(19.4) | 315(14.9) | 315(45.6) | 345(21.7) | 345(32.7) | 329(19.5) |
| [Y ₀ +H] ⁺ | 289(43.6) | 273(41.0) | 273(38.0) | 303(76.1) | 303(66.4) | 287(57.7) |
| [Y ₀ –H ₂ O+H] ⁺ | 271(21.7) | – | – | 285(7.7) | 285(12.0) | – |
| [Y ₀ –2H ₂ O+H] ⁺ | 253(6.4) | – | – | 267(1.7) | – | – |
| [Y ₀ –C ₂ H ₂ O+H] ⁺ | 247(4.6) | 231(1.1) | – | – | – | – |
| [A ₀ –B-ring+H] ⁺ | 179(50.4) | 179(1.1) | 179(9.3) | 179(62.1) | 179(66.3) | 179(27.0) |
| [^{1,3} A ₀ +H] ⁺ | 153(56.3) | 153(99.9) | 153(99.9) | 153(26.2) | 153(33.2) | 153(99.9) |
| [^{1,4} B–H ₂ +H] ⁺ | 163(99.9) | 147(43.9) | 147(38.0) | 177(99.9) | 177(99.9) | 161(64.4) |
| [^{1,3} B+H] ⁺ | 137(2.8) | – | 121(8.2) | 151(5.3) | 151(7.0) | 135(22.9) |
| Others | 171(15.9) | 171(14.6) | 171(44.6) | 171(8.7) | 171(16.4) | 171(45.4) |

3.3. Structural characterization of target compound

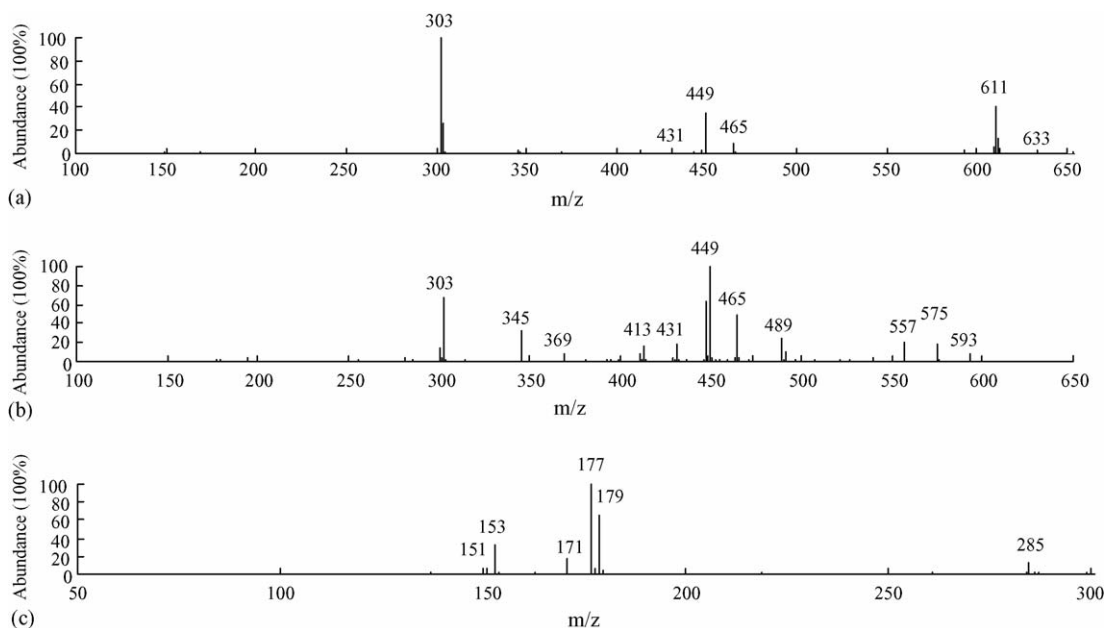
The total ion chromatogram (TIC) of treated sample of *F. aurantii* and standards hesperidin and naringin are shown in Scheme 4. Six target compounds were detected in TIC, the corresponding MS information are listed in Tables 3 and 4 for further structural characterization. Because peak 3 and peak 4 have identical RT and MS information as standards naringin and hesperidin, respectively, peak 3 was identified as naringin and peak 4 was identified as hesperidin. The mass spectra of compound 5 are shown in Scheme 5, which nearly has the same MS information

as hesperidin, although the abundance of the same product-ions is slightly different. Through those MS information, consulting literatures [18–20], compound 5 can be identified as neohesperidin. Similarly, compound 2 can be identified as isonaringin. Meanwhile, we find that the flavonoids with rutinose eluted prior to the corresponding flavonoids with neohesperidose, which is the same as those reported in literature [21].

The two isomeric pairs naringin and isonaringin as well as hesperidin and neohesperidin have alike structure and only differs by the interglycosidic linkage type between the two monosaccharides rhamnose and glucose. Hesperidin and isonaringin



Scheme 4. LC/MS total ion chromatogram: (a) treated sample of *Fructus Aurantii*; (b) standards naringin and hesperidin.

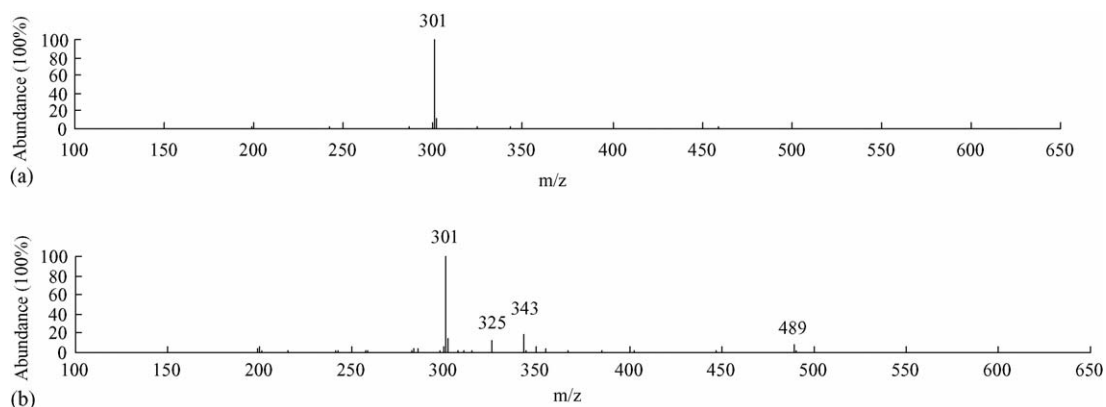


Scheme 5. The mass spectra of compound 5: (a) first order spectrum of compound 5; (b) CID-mass spectrum of protonated molecule of compound 5; (c) CID-mass spectrum of protonated aglycone of compound 5.

contains rutinose ([rhamnosyl-($\alpha 1 \rightarrow 6$)-glucose]) but neohesperidin and naringin contains neohesperidose ([rhamnosyl-($\alpha 1 \rightarrow 2$)-glucose]) (see Table 1). The CID-MS patterns of the isomer pair are so alike that cannot be used to distinguish them. Interestingly, there is little difference in the first order MS spectra between them. The relative abundance of Z_1 and Y_0 ions in isomeric pair are strikingly different. The $\alpha 1 \rightarrow 2$ linkage between the monosaccharides favors the elimination of the disaccharide residue to yield a protonated aglycone ion (Y_0), $Y_0 > Z_1$. However, $\alpha 1 \rightarrow 6$ linkage between the monosaccharides favors the elimination of the dehydrated glucose residue to yield a protonated flavonoid mono-*o*-glycosides ion (Z_1), $Z_1 > Y_0$. This feature was reported in literature [12] as a tool to distinguish the two most common interglycosidic linkage types between rhamnose and glucose, but the feature was observed in low-energy CID in their study. Using the same derivative process, peak 1 and peak 6 can rapidly be identified as neoeriocitrin and neoponcirin, respectively.

3.4. ESI(-)-MS analyse

In the structure analyse of flavonoid, spectra in positive ion mode are most frequently used, for which shows more extensive fragmentation than in negative ion mode. The fragmentation behaviors in negative ion mode are different, giving additional and complementary information. Though, in this study, the MS data obtained in positive mode have showed sufficient fragmentation and given us enough information to characterize the structure. The MS behaviors from negative ion mode provided additional information to differentiate the isomeric pair. Scheme 6 presents CID MS spectra for the deprotonated ion (m/z 609) of hesperidin and neohesperidin, respectively. As we can see from the spectra, the deprotonated molecule of hesperidin exhibits the only predominant fragment [Y_0-H] $^-$ (m/z 301). Whereas the deprotonated molecule of neohesperidin exhibits more fragments such as [$^{0,2}X_1-H$] $^-$ (m/z 489), [$^{0,2}X_0-H$] $^-$ (m/z 343), [$^{0,2}X_0-H_2O-H$] $^-$ (m/z 325), [Y_1-H] $^-$ (m/z 301). The iso-



Scheme 6. CID-mass spectra of deprotonated molecule of hesperidin and neohesperidin: (a) hesperidin; (b) neohesperidin.

pair p5-3. The same result exists between compound pair p3-1 and compound pair p6-5 in group 3. Thus, we conclude that the structural difference between homogenous compounds can be reflected quantitatively by their retention parameters, that is the same structural difference the same quantitative difference. The Δa , Δc and α values of compound pair p3-1 have a significant difference with the corresponding values of compound pair p6-5 in group 1, which do not accord with our conclusion. We consider the mechanism for this phenomenon is that the ortho-hydroxide radicals of aglycone of neoeriocitrin form inner molecular hydrogen bond, which influence the retention character of neoeriocitrin.

4. Conclusions

In present study, the structures of six flavanone *O*-diglycosides detected from the herb *F. aurantii*, were characterized on the basis of a partial interpretation of ESI-MS spectra. Our study demonstrated that the two most common (1,2- and 1,6-) interglycosidic linkages, e.g. flavonoid *O*-neohesperidosides and *O*-rutinosides can readily be differentiated on the basis of the first order ESI(+)-MS spectral data. The $\alpha 1 \rightarrow 2$ linkage between the monosaccharides favors the elimination of the disaccharide residue and yields a protonated aglycone ion (Y_0), $Y_0 > Z_1$. However, the $\alpha 1 \rightarrow 6$ linkage between the monosaccharides favors the elimination of the dehydrated glucose residue and yields a protonated flavonoid mono-*o*-glycosides ion (Z_1), $Z_1 > Y_0$. Meanwhile, the CID ESI(-)-MS spectra of the deprotonated ion have a distinct difference between the isomeric pairs. The $\alpha 1 \rightarrow 2$ linkage between the monosaccharides produces more fragments such as $[^{0,2}X_1-H]^-$, $[^{0,2}X_0-H]^-$, $[^{0,2}X_0-H_2O-H]^-$, $[Y_0-H]^-$. However, the $\alpha 1 \rightarrow 6$ linkage between the monosaccharides produces the only fragment $[Y_0-H]^-$. Through these two characteristic markers, the isomeric *O*-diglycosyl flavonoid pairs from the extract of *F. aurantii* can be readily differentiated. At the same time, the retention parameters a , c and k were obtained through UPLC experiments and a CSASS software. The relationship between structure and retention parameters was discussed and we found in a series of homogenous components, the difference of structures can be reflected quantitatively by their difference in retention parameters.

Acknowledgements

This work was supported by “Key project of National Science Foundation of China (20235020)” and “Key Project of Knowledge Innovation Program of Chinese Academy of Sciences (KGCX2-SW-213)”.

References

- [1] H. Smith, in: K. Mitrakos, W. Shropshire (Eds.), *Phytochrom*, Academic Press, London, 1972, pp. 433–434.
- [2] Y. Satoh, S. Tashiro, M. Satoh, Y. Fujimoto, J.Y. Xu, T. Ikekawa, *Yakugaku Zasshi* 116 (1996) 244–250.
- [3] Y.T. Huang, G.F. Wang, C.F. Chen, C.C. Chen, C.Y. Hong, M.C. Yang, *Life Sci.* 57 (1995) 2011–2020.
- [4] X.W. Zhao, J.X. Li, Z.R. Zhu, D.Q. Sun, S.C. Liu, *Chin. Med. J. (Engl.)* 102 (1989) 91–93.
- [5] D.Y. Zhou, Q. Xu, X.Y. Xue, F.F. Zhang, X. M. Liang, *Chin. J. Anal. Chem.*, in press.
- [6] P.Z. Lu, Y.K. Zhang, X.M. Liang, *High Performance Liquid Chromatography and its Expert System*, Publishing Company of Liaoning Technology, Shenyang, 1992, pp. 318–319.
- [7] P.Z. Lu, C.Z. Dai, X.M. Zhang, *Rationale of Chromatography*, Publishing Company of Sciences, Beijing, 1997, pp. 276–277.
- [8] S.L. Ge, J.Z. Tian, *Chin. Pharmacol. J.* 40 (2005) 365–367.
- [9] B. Domon, C.E. Costello, *Glycoconj. J.* 5 (1988) 397–403.
- [10] Y.L. Ma, Q.M. Li, H. Van den Heuvel, M. Claeys, *Rapid Commun. Mass Spectrom.* 11 (1997) 1357–1364.
- [11] Y.L. Ma, I. Vedernikova, H. Van den Heuvel, M. Claeys, *J. Am. Soc. Mass Spectrom.* 11 (2000) 136–144.
- [12] Y.L. Ma, F. Cuyckens, H. Van den Heuvel, M. Claeys, *Phytochem. Anal.* 12 (2001) 159–165.
- [13] F. Cuyckens, R. Rozenberg, *J. Mass Spectrom.* 36 (2001) 1203–1210.
- [14] F. Cuyckens, M. Claeys, *J. Mass Spectrom.* 39 (2004) 1–15.
- [15] U. Justesen, *J. Mass Spectrom.* 36 (2001) 169–178.
- [16] C.W. Huck, C.G. Huber, K.-H. Ongania, G.K. Bonn, *J. Chromatogr. A* 870 (2000) 453–462.
- [17] P. Dugo, L. Mondello, L. Dugo, R. Stancanelli, G. Dugo, *J. Pharm. Biomed. Anal.* 24 (2000) 147–154.
- [18] K. Robards, X. Li, M. Antolovich, S. Boyd, *J. Sci. Food Agric.* 75 (1997) 87–101.
- [19] P. Dugo, M.L. Presti, M. Ohman, A. Fazio, G. Dugo, L. Mondello, *J. Sep. Sci.* 28 (2005) 1149–1156.
- [20] P. Swatsitang, G. Tucker, K. Robards, D. Jardine, *Anal. Chim. Acta* 417 (2000) 231–240.
- [21] X.G. He, L.Z. Liang, L.Z. Lin, W.B. Matthew, *J. Chromatogr. A* 791 (1997) 127–134.